Teknomekanik, Vol. 5, No. 2, pp. 90-96, December 2022
e-ISSN: 2621-8720 p-ISSN: 2621-9980

Cellulose derivative as protection coating: Effect of nanoparticle additives on load capacity

Shih-Chen Shi* and Xiao-Ning Tsai

Department of Mechanical Engineering, National Cheng Kung University, Tainan 70101, TAIWAN

*Corresponding Author: scshi@mail.ncku.edu.tw
Received Sep 07th, 2022; Revised Oct 28th, 2022; Accepted Nov 07th, 2022
DOI: https://doi.org/10.24036/teknomekanik.v5i2.16372

ABSTRACT

The cellulose derivative Hydroxypropyl Methylcellulose (HPMC) has recently been extensively studied and used in mechanical applications. However, the softness and susceptibility to deformation of HPMC limited its further applications. In this study, metal nanoparticles (nano-aluminum and nano-copper) and nano-metal oxide particles (nano-alumina and nano-copper oxide) were used as additives to HPMC to form a composite film with improved mechanical properties, particularly load capacity. The addition of high levels of additives provided a higher load capacity. Among the nano-additives used in the study, Cu (2 wt.%) provided the composite with the highest load capacity, improving the load capacity of pure HPMC by 250%. The surface treatment of strengthening additives is an important step. Adding specific high-strength and high-modulus metal and metal oxide additives to the soft HPMC matrix can effectively improve the load-bearing capacity of the composite material. This study proposes a simple evaluation method for the load-bearing capability of the coating as well.

Keywords: Load capacity; Nanoparticle additive; Cellulose composite; Coating.

How to Cite:

S.-C. Shi and X.-N. Tsai, "Cellulose derivative as protection coating: Effect of nanoparticle additives on load capacity", *Teknomekanik*, vol. 5, no. 2, pp. 96-102, Dec. 2022.
https://doi.org/10.24036/teknomekanik.v5i2.16372

1. INTRODUCTION

The development of polymer–nanoparticle composites has been ongoing since the 1900s. As nanoparticles tend to have a large number of surface defects and strong Van der Waals forces, their incorporation into polymers often increases strength and resistance to pressure and wear. Currently, many domestic products have been improved through the use of polymer–nanoparticle composites. For instance, the mechanical properties of vulcanized rubber are significantly improved by the incorporation of carbon black, zinc oxide, and magnesium sulfate. The binding of carbon black to the elastomer matrix leads to the formation of a carbon gel with a networked structure [1], [2], which increases the tensile strength, hardness, and wear resistance of the rubber product. At present, nearly all tires, conveyer belts, and rubber hoses are made from composites containing carbon black. Many researchers have sought to design polymer–nanoparticle composites that could be used as engineering materials, but a multitude of obstacles have emerged during this process. One of the key challenges faced by researchers is the difficulty of creating a uniform dispersion of nanoparticles within an elastomer matrix without causing aggregation using cost effective methods. Several studies attributed the mechanical improvement caused by the addition of inorganic particles to a polymer to various reasons. Although inorganic nanoparticles innately possess high stiffnesses, the stiffness and Young's modulus of the composite actually depends on stress transfer between the matrix and additive [3]. If there is an effective path for stress transfer from the matrix to the additive, the additive can then significantly improve the mechanical properties of the composite. However, aggregation increases the effective size of the nanoparticle additive and thus nullifies the size effect and surface effect of the additive. Furthermore, the weak bonding of the aggregates to the matrix causes defects that weaken the mechanical properties of the composite [4], [5]. Therefore, designing effective and practical nanoparticle dispersion methods is important for the further development of polymer–nanoparticle composites [4].

Composites based on biopolymer matrices have become very important in recent years [6], [7]. Due to their low density, excellent biocompatibility, ubiquity, and environmental friendliness, biopolymers have been

applied in a wide variety of areas, including sustainable manufacturing [8], [9], dry tribological coatings [10], [11], anti-corrosion coatings [12], [13], and impact resistant materials. Furthermore, due to the abundance of hydroxyl groups on the surface of biopolymers, some biopolymer-based composites are capable of self-healing in certain environments [14]. Many biopolymer-based composites, however, have low mechanical strength. Therefore, many strength-enhancing additives have been used in these composites, including graphite [15], molybdenum disulfide [16], and metal/metal oxide nanoparticles [17].

The goal in developing composite materials is usually to enhance a specific property of interest. For instance, composites used in machinery usually have enhanced mechanical properties to enable their use as protective layers or in anti-wear applications. It is hypothesized that the addition of nanoparticles, which have much higher Young's moduli and maximum tensile strengths than cellulose derivatives, can enhance the mechanical properties and load capacity of hydroxypropyl methylcellulose (HPMC) films. However, related studies are pretty few. This study's importance lies in providing a composite material fabrication process for cellulose-based biopolymer composites. This work proposes a new simple method to measure the load capacity of a biopolymer composite.

2. MATERIAL AND METHODS

The nanoparticle-enhanced HPMC films were prepared in four steps: (1) Preparation of the HPMC solution: An 8:2 mixture of 95% ethanol and deionized water (100 g) was heated to 60 °C on a magnetic stirring hotplate. HPMC powder (10 g; USP-2910 PHARMACOAT 606, Shin-Etsu, Tokyo, Japan) was added to the mixture and then cooled to room temperature while stirring rapidly. After fully dissolving the HPMC powder, the solution was transparent and colorless. (2) Preparation of the nanoparticle suspension: Citric acid (SFL Beauty & Chem, Tainan, Taiwan) was mixed with nanoparticles (Al, Al_2O_3, Cu, CuO) in a 1:1 ratio. The nanoparticles mixture (0.2 g and 0.4 g) was then dissolved in ethanol (10 g) and then heated to 60 °C using a magnetic stirring hotplate. Finally, Span 80 in ethanol was added to the mixture and then ultrasonicated for 10 min. (3) Preparation of the composite solution: The HPMC solution and nanoparticle suspension were mixed in a 1:1 ratio to form a 20 g solution, which was magnetically stirred at 400 rpm. (4) Preparation of the nanoparticle-enhanced HPMC film: The composite film was prepared via solution evaporation. The composite solution (486 µL) was dropped onto a K_2O-B_2O_3-S_iO_2 plate (Paul Marienfeld, Lauda-Königshofen, Germany). The coated plate was then placed in an environment with a temperature of 25 °C and a relative humidity of 45% for 6 h.

The surface morphologies of the composite films were observed via scanning electron microscopy (SEM). The indentations and their depths were measured using a 3D laser scanning microscope. The hardness of each film was measured by indenting the film using a standardized steel ball indenter (indenter diameter, D = 10 mm) for 30–60 s, with the load P being varied according to the hardness of the film. After the indenter was removed, a microscope was used to measure the two diagonal lengths of the indentation, which were averaged to obtain the indentation diameter, d. The Brinell hardness of the film was determined by dividing P by the area of indentation. In ISO standards 6506-1 and ISO 6506-2:2005, any measurement of Brinell hardness must satisfy the following constraints: (1) The thickness of the specimen must be at least 10 times that of the indentation. (2) The center-to-center distance between two indentations must be at least 4 times the indentation diameter. (3) The distance between an indentation center to the edge of the material must be at least 2.5 times the indentation diameter. Therefore, Brinell hardness tests are only suitable for large specimens.

$$HB = \frac{\mathrm{P}}{\pi D t} = \frac{2\mathrm{P}}{\pi \mathrm{D}(\mathrm{D}-\sqrt{D^2-d^2})} \quad (1)$$

where P is the load in kg, D is the indenter diameter in mm, and d is the indentation diameter in mm.

Load capacity (kgf/mm^2) was measured using a modified version of the Brinell hardness test. The measurement system is shown in Figure 1. An AISI 52100 chrome steel ball (D = 3/32") was used as the indenter. By varying the weight of the glass bottle, the film was indented with a force of 15 N (1.53 kg) for 3 min and 20 N (2.04 kg) for 30 s. After the indentations were made, the four corners and center point of each specimen were measured. Thereafter, the specimens were indented first and then left to stand for 12 h to avoid errors caused by short-term rebounding. A 3D laser scanning microscope was then used to observe the indentations. Load capacity was computed from the diameter and depth of the indentations using Equation (1), which is a modified formula for Brinell hardness. It was observed that the film piled up at the edges of each indentation due to the severe plastic deformation that occurs during the indentation test. As this may affect measurement accuracy, indentation diameter and depth were derived from the laser-scanned contour of each indentation instead of the direct indentation and length measurements obtained using the microscope.

Figure 1: Measurement system for load capacity measurements

3. RESULTS AND DISCUSSION

Figure 2 shows the surface morphologies of four different HPMC films with different types and amounts of additives, and Figure 3 shows the surface roughness of the composite films. As shown in Figures 2 and 3, the nanoparticle coverage and surface roughness of the composite films both increase with increasing nanoparticle addition. We speculate that these macroscopic changes were due to solvent evaporation during the formation of the composite film, which caused some of the nanoparticles to become exposed on the surface of the films, forming rough peaks. In formulations where the nanoparticle volume fraction in the solution is high, the nanoparticles within the solution may come in contact with each other and aggregate due to the decreasing volume of solvent, increasing surface roughness. Generally, the aggregates that formed in the HPMC composites with 2 wt.% of nanoparticle additives were larger than those formed with 1 wt.% of nanoparticle additives.

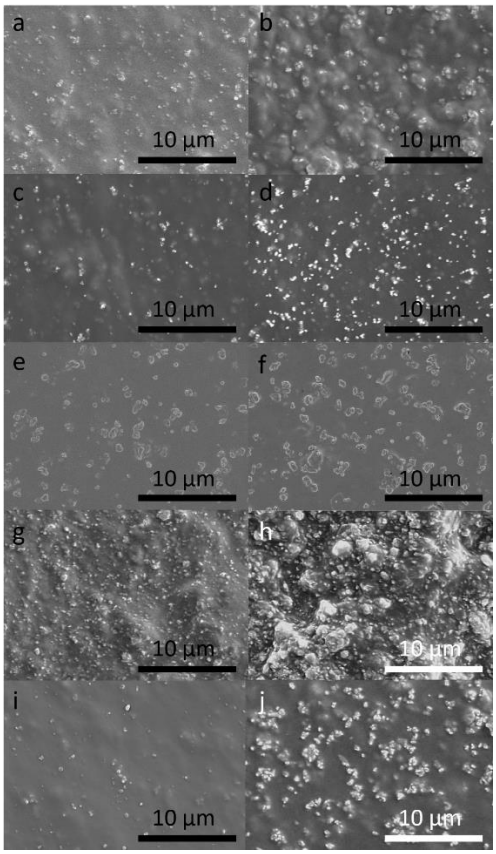

Figure 2: Surface SEM micrographs of the composite films with different types and amounts of nanoparticle additives. (a) Al 1%, (b) Al 2%, (c) Cu 1%, (d) Cu 2%, (e) Al_2O_3 ball 1%, f) Al_2O_3 ball 2%, (g) Al_2O_3 rod 1%, (h) Al_2O_3 rod 2%, (i) CuO 1%, (j) CuO 2%

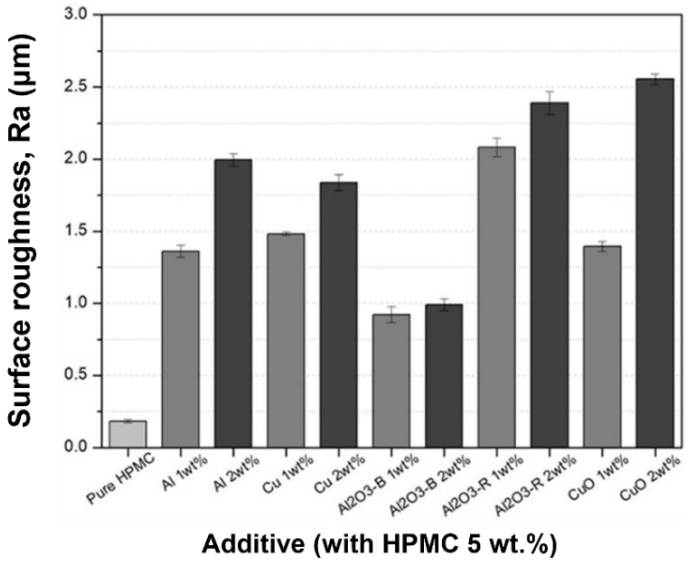

Figure 3: Surface roughness of the composite films

Figure 4 shows the width of the indentation marks left by a 3/32" chrome steel indenter after 3 min of loading at 15 N on pure HPMC, the HPMC composite films, and a 2.7-mm-thick polypropylene (PP) film with a hardness of 8 kgf/mm^2. The indentation width of PP and pure HPMC were 496 µm and 508 µm, respectively. All of the nanoparticle additives improved the mechanical properties of HPMC, as evidenced by the reduction in the indentation width relative to pure HPMC, but in varying degrees. We speculate that this is caused by the variations in particle type and size, which results in different levels of surface adhesion. As a result, nanoparticle-matrix binding differs from one type of nanoparticle to another. It was also found that for each type of nanoparticle, 2 wt.% of nanoparticle addition always resulted in a lower indentation width than 1 wt.% of nanoparticle addition.

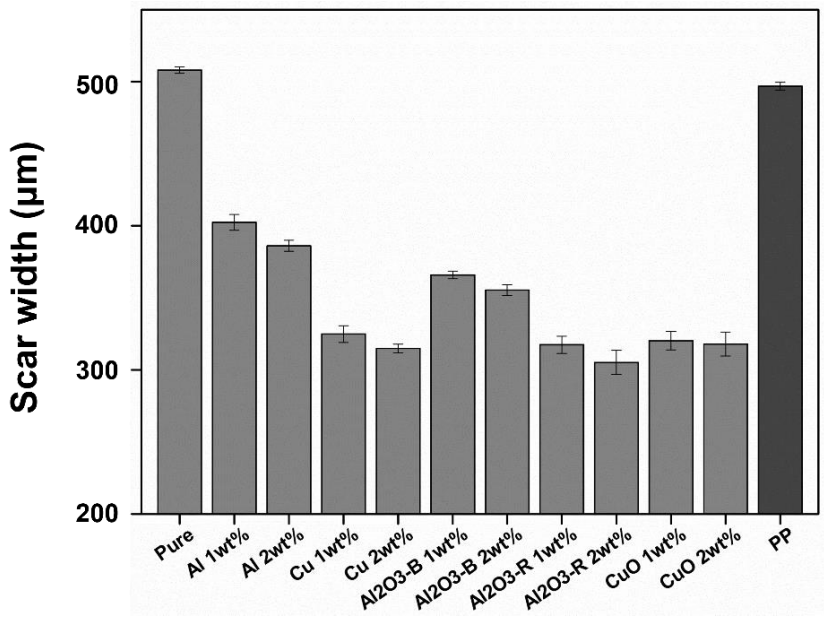

Figure 4: Width of indentation on various films (15 N load with 3/32" AISI 52100 chrome steel ball for 30s)

Figure 5 shows the load capacities calculated using Equation (1), based on the widths of the indentations formed by a 3/32" chrome steel ball indenter after loading 20 N for 30 s. The load capacity of pure HPMC was found to be 9.6 kgf/mm^2. The largest improvement in load capacity was observed in the composite film with 2 wt.% Cu additives. Although the improvement in mechanical performance due to nanoparticle addition does depend on the intrinsic mechanical properties of the matrix and the additives, it is more significantly affected by the efficiency of stress transfer from the matrix to the additive during loading. Therefore, the interfacial

bond strength between the matrix and additive is a more important factor for additive-induced improvements to mechanical performance.

The reason why Cu outperformed the other types of nanoparticle additives could be attributed to the citric acid wash during the preparation of the nanoparticle solution. This step reactivates the surfaces of the Cu nanoparticles and thus improves their adsorption to the HPMC matrix if their dispersion within the HPMC matrix is uniform. Nonetheless, load capacity is generally improved by nanoparticle addition, and such improvement commonly increases with the nanoparticle concentration. Therefore, it may be concluded that the nanoparticles in the composite film will always bear a portion of the load, regardless of their type.

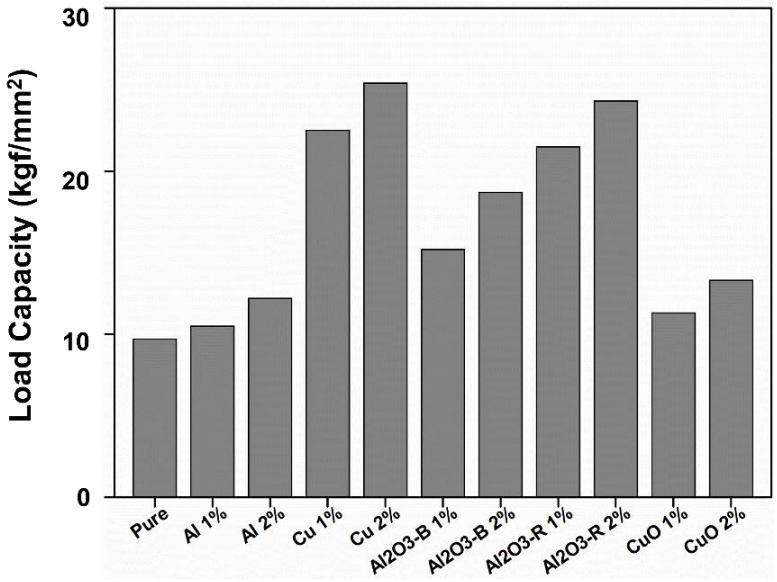

Figure 5: Load capacity of the composite films (20 N load with 3/32" AISI 52100 chrome steel ball for 30s)

Figures 6 and 7 show the load curves and load capacities of all of the composite films, respectively. Here, the actual contact area between the indenter and film corresponds to the area that exhibits deformed surface asperities. Comparing the 2 wt.% composite films with non-additive pure HPMC, it is clear that the latter has lower load capacities. Therefore, the actual contact area of the pure HPMC films must be larger than wt.% composite films.

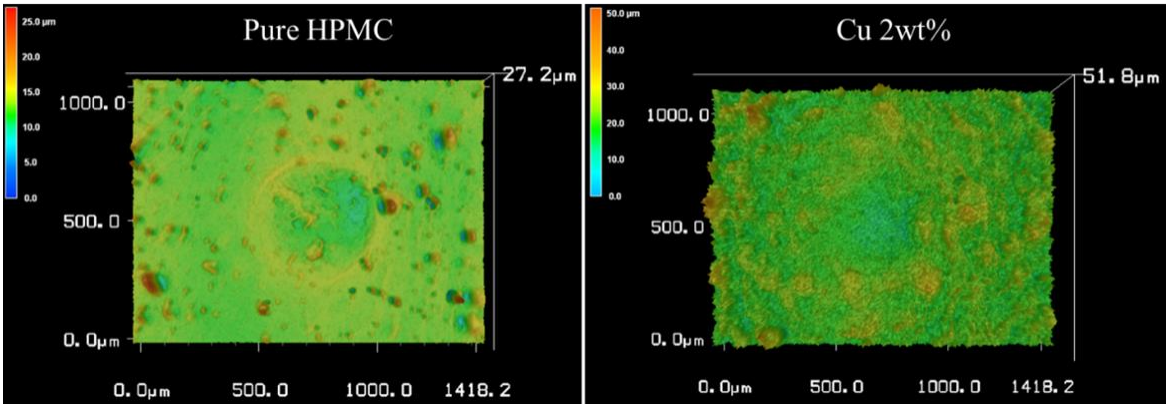

Figure 6: 3D-laser-scanned features of the indentation on two different films (20 N load with a 3/32" AISI 52100 chrome steel ball for 30 s)

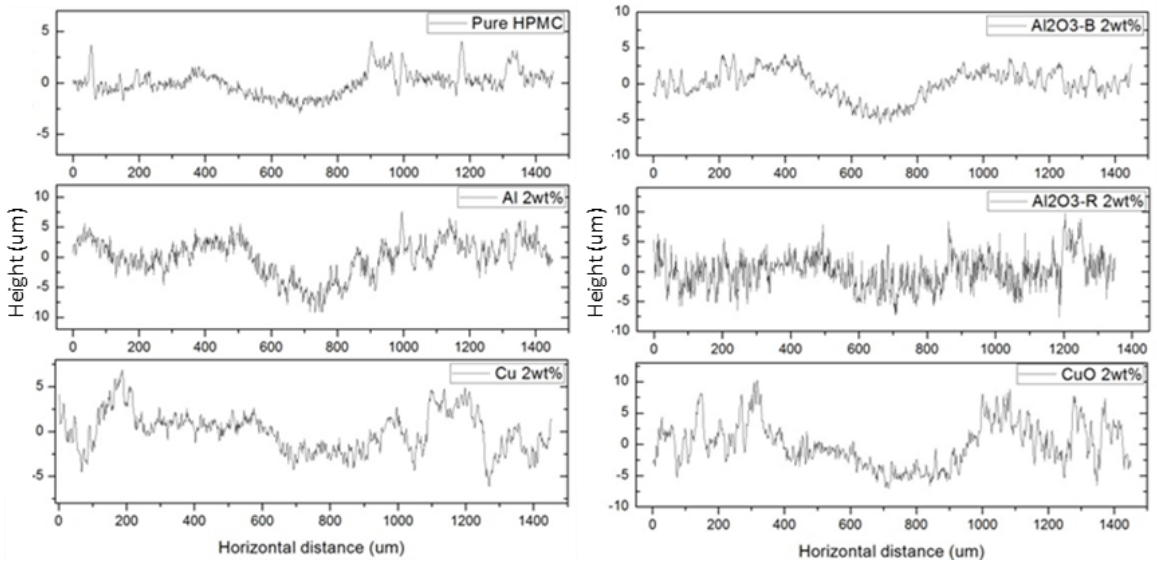

Figure 7: Cross-sectional curves of the indentation on each composite film (20 N load with a 3/32" AISI 52100 chrome steel ball for 30 s)

There is rarely relevant literature discussing the load resistance capacity of biopolymer dry coatings. Therefore, the discussion in this study is based on the additive properties' influence on the coating's load resistance. The presence of nanoparticles inside the composite film can bear a specific load. Therefore, the composite film with a higher concentration has a better load capacity. However, in the same weight percentage concentration, the volume percentage of aluminum particles is greater than that of copper particles. However, in terms of the material's mechanical properties, copper's yield strength is more significant than aluminum's (69 MPa > 35 MPa). Therefore, the copper-additive composite film has a higher load capacity than the aluminum-additive composite. Likewise, aluminum oxide has a higher compressive strength than copper oxide, so it performs better in the load-bearing capacity of the composite.

4. CONCLUSION

Various of nanoparticle/HPMC composite films were prepared by adding Al, Cu, Al_2O_3, or CuO nanoparticles to HPMC, with Span 80 as the dispersant. The morphological and mechanical properties of these films were then investigated. It was found that nanoparticle addition generally improved load capacity and that higher nanoparticle concentrations generally led to higher load capacities. The composite film with 2 wt.% of Cu additives showed the largest improvement in load capacity. In all the composite films, the metallic/non-metallic nanoparticles could bear loads to some extent. The extent to which nanoparticle addition improves the mechanical properties of a composite film mainly depends on the nanoparticle-matrix interfacial bond strength. However, only a small amount of addition was used in this article, and the effect of more additions is worthy of further study.

ACKNOWLEDGEMENTS

This work was supported by the National Science and Technology Council, Taiwan (grant number MOST 110-2221-E-006-150, 111-2221-E-006-145, 111-2221-E-006-147-MY2, and 111-2221-E-006-133). The authors gratefully acknowledge using EM000700 of MOST 110-2731-M-006-001 belonging to the Core Facility Center of National Cheng Kung University.

DECLARATIONS

Author contribution

S.C Shi: Writing - Original Draft, Conceptualization, Formal analysis, Resources, Visualization, Supervision. X.N Tsai: Writing -Review & Editing, Conceptualization, Formal analysis, Investigation.

Funding statement

This work was supported by the National Science and Technology Council, Taiwan (grant number MOST 110-2221-E-006-150, 111-2221-E-006-145, 111-2221-E-006-147-MY2, and 111-2221-E-006-133).

Competing interest

The authors declare that they have no known competing financial interests or personal relationships that could have appeared to influence the work reported in this paper.

REFERENCES

[1] B. B. Boonstra, "Role of particulate fillers in elastomer reinforcement: a review," *Polymer*, vol. 20, no. 6, pp. 691–704, Jun. 1979, https://doi.org/10.1016/0032-3861(79)90243-X

[2] N. Kida, M. Ito, F. Yatsuyanagi, and H. Kaido, "Studies on the structure and formation mechanism of carbon gel in the carbon black filled polyisoprene rubber," *J Appl Polym Sci*, vol. 61, no. 8, pp. 1345–1350, Aug. 1996, https://doi.org/10.1002/(SICI)1097-4628(19960822)61:8<1345::AID-APP15>3.0.CO;2-Y

[3] S. C. Shi, T. H. Chen, and P. K. Mandal, "Enhancing the Mechanical and Tribological Properties of Cellulose Nanocomposites with Aluminum Nanoadditives," *Polymers 2020, Vol. 12, Page 1246*, vol. 12, no. 6, p. 1246, May 2020, https://doi.org/10.3390/polym12061246

[4] S. C. Shi and X. X. Zeng, "Effect of the strengthening mechanism of SiO2 reinforced poly(methyl methacrylate) on ductility performance," *Journal of Polymer Research 2022 29:10*, vol. 29, no. 10, pp. 1–9, Sep. 2022, https://doi.org/10.1007/S10965-022-03259-0

[5] T. Jiang, T. Kuila, N. H. Kim, B. C. Ku, and J. H. Lee, "Enhanced mechanical properties of silanized silica nanoparticle attached graphene oxide/epoxy composites," *Compos Sci Technol*, vol. 79, pp. 115–125, Apr. 2013, https://doi.org/10.1016/j.compscitech.2013.02.018

[6] K. P, S. v S, and B. N. Narayanan, "Ball-Mill Assisted Green One-Pot Synthesis of ZnO/Graphene Nanocomposite for Selective Electrochemical Sensing of aquatic pollutant 4-nitrophenol," *Teknomekanik*, vol. 4, no. 2, pp. 64–71, Oct. 2021, https://doi.org/10.24036/teknomekanik.v4i2.10872

[7] J. L. Ardi, H. Nurdin, A. Arafat, and S. R. P. Primandani, "Analysis of Tensile Strength of Citronella (Cymbopogon Nardus) Fiber Reinforced Composite Materials," *Teknomekanik*, vol. 4, no. 2, pp. 72–77, Oct. 2021, https://doi.org/10.24036/teknomekanik.v4i2.10472

[8] S. C. Shi and F. I. Lu, "Biopolymer Green Lubricant for Sustainable Manufacturing," *Materials 2016, Vol. 9, Page 338*, vol. 9, no. 5, p. 338, May 2016, https://doi.org/10.3390/ma9050338

[9] S. C. Shi and T. F. Huang, "Raman study of HPMC biopolymer transfer layer formation under tribology test," *Optical and Quantum Electronics 2016 48:12*, vol. 48, no. 12, pp. 1–9, Nov. 2016, https://doi.org/10.1007/S11082-016-0807-4

[10] S. C. Shi and Y. Q. Peng, "Preparation and tribological studies of stearic acid-modified biopolymer coating," *Prog Org Coat*, vol. 138, p. 105304, Jan. 2020, https://doi.org/10.1016/j.porgcoat.2019.105304

[11] S. C. Shi and J. Y. Wu, "Deagglomeration and tribological properties of MoS2/hydroxypropyl methylcellulose composite thin film," *Surf Coat Technol*, vol. 350, pp. 1045–1049, Sep. 2018, https://doi.org/10.1016/j.surfcoat.2018.02.067

[12] S. C. Shi and C. C. Su, "Electrochemical behavior of hydroxypropyl methylcellulose acetate succinate as novel biopolymeric anticorrosion coating," *Mater Chem Phys*, vol. 248, p. 122929, Jul. 2020, https://doi.org/10.1016/j.matchemphys.2020.122929

[13] S. C. Shi, "Hydroxypropyl Methylcellulose Phthalate Biopolymer as an Anticorrosion Coating," *Int J Electrochem Sci*, vol. 16, pp. 1–10, 2021, https://doi.org/10.20964/2021.09.44

[14] S. C. Shi and T. F. Huang, "Effects of temperature and humidity on self-healing behaviour of biopolymer hydroxylpropyl methylcellulose for ecotribology," *Surf Coat Technol*, vol. 350, pp. 997–1002, Sep. 2018, https://doi.org/10.1016/j.surfcoat.2018.03.039

[15] S. C. Shi and S. Z. Jiang, "Influence of graphene/copper hybrid nanoparticle additives on tribological properties of solid cellulose lubricants," *Surf Coat Technol*, vol. 389, p. 125655, May 2020, https://doi.org/10.1016/j.surfcoat.2020.125655

[16] S. C. Shi, X. N. Tsai, and S. S. Pek, "Tribological behavior and energy dissipation of hybrid nanoparticle-reinforced HPMC composites during sliding wear," *Surf Coat Technol*, vol. 389, p. 125617, May 2020, https://doi.org/10.1016/j.surfcoat.2020.125617

[17] S. C. Shi and J. H. C. Yang, "Preparation of stable biopolymer composite suspension with metal/metal-oxide nanoparticles," *Modern Physics Letters B*, vol. 34, no. 7–9, Mar. 2020, https://doi.org/10.1142/s021798492040028x